JOURNAL OF THERMOPHYSICS AND HEAT TRANSFER
Vol. 12, No. 2, April–June 1998

Review of the Thermal Conductivity of Thin Films

S. R. Mirmira* and L. S. Fletcher†
Texas A&M University, College Station, Texas 77843-3123

The thermal conductivity of thin films (0.01–100 μm) governs the heat transfer characteristics and affects the performance and reliability of the microelectronic devices in which they are used. To measure the thermal conductivity of these films, several different steady-state and transient techniques have been developed, some involving the use of lasers. New methods of thin-film deposition have also been developed. This paper reviews experimental and analytical techniques and the thermal conductivity results obtained. It is shown that that the results obtained by these different measurement techniques and deposition methods vary significantly. This emphasizes the importance of measuring the thermal conductivity of thin-film materials that closely resemble those being used in specific applications.

Nomenclature

A = cross-sectional area
a = radius of film
b = width
C = specific heat
d = diameter of metal line
E = exponential function
e = electrical charge
ef = thermal diffusivity
f = frequency
G = conductance
g = ratio of film to substrate effusivity
I = electrical current
K = thermal conductivity
k = Boltzmann constant
L = location of film edge
L_o = Lorentz constant
l = length of line
N = number of slabs of coating material
q = power output–input length
R = resistance
T = temperature
t = time
W = width
X = location of sensor
z = layer of thickness
α = thermal diffusivity
α' = thermal conductivity of microcracks
β = size of microcracks
γ = fraction cross-sectional area covered by microcracks, $\gamma < 1$
Δ = difference
ε = emissivity
λ = mean free path of phonons
ν = velocity of sound
ρ = density
σ = electrical conductivity
τ = time constant
ω = frequency

Subscripts
app = apparent
av = average
B = boundary
CR = thermal conduction and radiation
c = critical
cond = conduction
eff = effective
el = electrical contribution
f = film
i = integer
int = internal
la = lattice
m = microcracks
n = net
o = ambient
p = pressure
rad = radiation
s = substrate
slab = slabs of coating material
th = thermal

Introduction

KNOWLEDGE of thermophysical properties, such as thermal conductivity and thermal diffusivity, of thin films is extremely important from the standpoint of heat transport during the nucleation and growth of such films, as well as in the technological applications of these films. During the use of thin films in devices such as laser diodes and integrated transistor circuits, the heat generated needs to be rapidly dissipated and, hence, the thermal conductivity and diffusivity of the film plays an important role.

It has been demonstrated that the thermal conductivity of thin films may differ significantly from the bulk values, because of microstructural differences as well as differences in the phonon transport mechanisms between thin films and the bulk material. Several different techniques have been developed to measure and predict the thermal conductivity of thin-film materials. In the last decade, significant advances have been made in the field of microscale heat transfer that have led to state-of-the-art review articles. Cahill[1] published a review article on the heat transport mechanisms in dielectric thin films. The article discusses a few of the experimental and theoretical studies of heat transport by lattice vibrations in thin-film materials. Goodson and Flik[2] conducted a review of steady-state and transient measurement techniques employed in the measurement of thermal conductivity parallel and perpendicular to solid layers. The review concludes that a more detailed uncertainty analysis is required for most of the tech-

Received May 27, 1997; revision received Oct. 3, 1997; accepted for publication Oct. 6, 1997.

*Graduate Research Assistant, Conduction Heat Transfer Laboratory, Mechanical Engineering Department. Student Member AIAA.

†Thomas A. Dietz Professor, Conduction Heat Transfer Laboratory, Mechanical Engineering Department. Fellow AIAA.

niques employed. Graebner[3] and Blanchard et al.[4] conducted extensive reviews on measurement techniques and results on the thermal conductivity of diamond films. Chen and Tien[5] published an article on the effects of size and boundary of gallium arsenide-based quantum well structures. Their results show that the thermal conductivity of the quantum well may be an order of magnitude lower than the bulk form. The present review discusses both analytical and experimental (steady-state and transient) techniques recently developed to measure the thermal conductivity of thin films.

Literature Review

Inasmuch as there are a wide range of techniques used to determine the thermal conductivity of thin films, comparisons can be made only in the context of similar techniques. Therefore, this review will categorize the studies in terms of experimental and analytical techniques. The various experimental models are expanded on in Table 1, and the analytical models are detailed in Table 2.

Experimental Techniques

Okuda and Ohkubo[6] developed an experimental technique to measure the thermal conductivity of dielectric films down to a few hundred nanometers in thickness. In this technique, a very narrow metal line was produced on the thin-film surface by using a photolithography technique. By observing the rate at which the temperature of the metal line increased within a very short period of time (microsecond), it was possible to accurately obtain the thermal conductivity of the substance under the wire line. A schematic of the experimental geometry is shown in Fig. 1. By assuming the heat capacity of the wire line to be negligible, the temperature change $\Delta T(t)$ for a line of width $2d$ was obtained. The thermal conductivity was calculated from $\Delta T(t)$, which was determined by measuring the resistance in the line, and from the calculated q and τ. Table 1 lists the expression developed by Okuda and Ohkubo.[6]

The success of this technique depends upon the metal line being very narrow, and the transient measurement being conducted with extremely high time resolution. The drawback associated with this technique is that the heat capacity of the metal line cannot be neglected because very often the thickness of the line is comparable to the film thickness. When the heat capacity of the line is considered, the theory is extremely complex and has not been completely worked out.

Okuda and Ohkubo[6] used this technique to measure the thermal conductivity of silicon dioxide films 0.1–1 μm in thickness. The thermal conductivity exhibited no significant change over this thickness range. The data are shown in the Results section.

Table 1 Experimental models for thermal conductivity of thin films

Investigator	Expressions	Remarks
Okuda and Ohkubo[6]	$K = -\left[\frac{q}{A(\Delta T/\Delta l)}\right]$, $q = \frac{I^2R}{l}$, $\tau = \frac{(\alpha t)^{1/2}}{d}$, $\Delta T = \frac{q}{\pi^{1/2}K}\left[1 - \exp\left(\frac{-1}{\tau^2}\right) - \frac{1}{2\pi^{1/2}} Ei\left(\frac{-1}{\tau^2}\right)\right]$	1) Success depends on metal line being narrow. 2) Extremely high time resolution required. 3) Neglects heat capacity of metal line. 4) Used for SiO_2 thin films.
Cahill et al.[7]	$K = (q^{-1})(\sqrt{2\rho C_p \omega})$, $\lvert q^{-1}\rvert = \left(\frac{\alpha}{2\omega}\right)^{1/2}$	1) 3ω technique applicable for film thickness of 10 μm and greater. 2) Insensitive to radiative losses.
Cahill et al.[7]	$K = \frac{d}{R_B}$ $R_B = \frac{\Delta T}{q/A}$	1) Used for film thickness less than 10 μm. 2) Thermal conductivity is calculated by knowing the thermal boundary resistance.
Zhang and Grigoropoulos[14]	$k = \frac{q}{\Delta T}(L - X)$	1) Freestanding thin films. 2) Film edge is assumed to be at room temperature. 3) Used for Si–N films.
Lambropoulos et al.[16]	$\frac{1}{K_{eff}} = \frac{\pi}{4}\frac{a}{d}\left(\frac{1}{K_{app}} - \frac{1}{K}\right)$ for $d \ll a$ $\frac{1}{K_{app}} = \frac{1}{K_{eff}} + \frac{8}{\pi}\frac{1}{K_{eff}}\sum_{n=1}^{\infty}\theta^n I_n\left(\frac{d}{a}\right)$ for $d \approx a$ $\theta = \frac{(K_{eff}/K_s) - 1}{(K_{eff}/K_s) + 1}$	1) Apparent thermal conductivity of film–interface assembly is obtained from the calibration curve. 2) Expressions show the explicit dependence of K_{eff} on K_{app} and the ratio of d/a. 3) Plot of d vs K_{eff} yields K_f^{-1}.
Völklein[17]	$K_f = K_{SiO_2}d_{SiO_2} + 2K_{Si_3N_4}d_{Si_3N_4}$ $\Delta T = \frac{q}{G_{CR} + G_{RB}}\left[1 - \frac{2}{\nu b}\tanh\left(\frac{\nu b}{2}\right)\right]$	1) Steady state. 2) Advantages of sandwich system are its small thickness and high thermal stability, which permits investigation of thin film deposited at high temperatures.
Goodson et al.[22] and Käding et al.[24]	$R_{th}(d) = \frac{d}{K_{int}(d)} + R_{B1} + R_{B2}$	1) Imperfections in the SiO_2 layer are accounted for in $d/K_{int}(d)$. 2) Adhesion to and microstructure of the metal is accounted for in R_{B2}. 3) Incomplete adhesion of oxide is accounted for in R_{B1}. 4) Not valid for very thin films and at very low temperatures.
Graebner et al.[25,26]	$K = \frac{q}{A(dT/dl)}$, $A = ZW$ $\frac{K_{rad}}{K_{cond}} = \frac{2\varepsilon\sigma W^2 T_0^3}{K d}$	1) The temperature gradient is adjusted to account for radiative losses. 2) The maximum value of the ratio (radiated to conducted heat) was 0.25, implying an error of 25% if radiation is neglected.
Graebner et al.[29]	$K = \rho\alpha C_p$ $\Delta T(t) = (\Delta T)_{max}\left[1 + 2\sum_{n=1}^{\infty}(-1)^n \exp\left(\frac{-n^2\pi^2\alpha t}{d^2}\right)\right]$	1) Method utilizes a high-speed laser technique. 2) A nonlinear least-squares fit of transient temperature response yields values for α.

Table 2 Analytical models for thermal conductivity of thin films

Investigator	Expressions	Remarks
Ziman[32]	$K = \frac{1}{3}(Cv\lambda)$	1) Accounts for phonons of all frequencies. 2) Neglects energy dependence of the carrier free paths.
Anderson[33]	$K_{el} = \sigma L_O T, \quad L_O = \frac{\pi^2}{3}\left(\frac{k}{e}\right)^2, \quad K_{la} = \frac{1}{3}(Cv\lambda)$	1) Wiedemann–Franz law is applicable to only electrically conducting materials. 2) For bulk materials, the lattice component is negligible.
Redondo and Beery[35]	$\frac{K_n}{K} = \left[1 + \frac{(N_{slab} - 1)(1 - K_n)\beta\gamma}{1 - (1 - K_n)\gamma}\right]$ microcrack model	1) Model assumes thin-film coatings contain microcracks. 2) Model predicts that imperfections may cause reductions on the order of 2 or more orders in thermal conductivity.
	$\frac{K_n}{K} = 1 - (1 - K_c)\gamma$ Swiss cheese model	3) Model suggests a possible mechanism for laser-induced damage of optical coatings.
Swimm[36]	$K = \left(\frac{e^2}{\sqrt{\rho C_p}}\right), \quad f_c = \left(\frac{\alpha_f}{l_f^2}\right), \quad g = \frac{e_s}{e_f}$	1) Requires knowledge of bulk material properties. 2) g and f_c are calculated from phase differences.

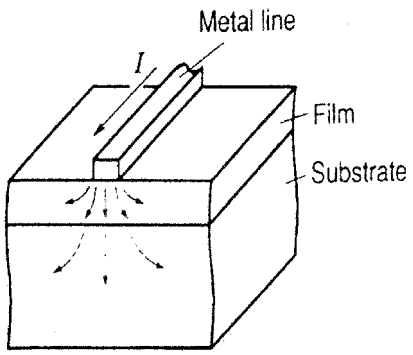

Fig. 1 Schematic of experimental geometry.[6]

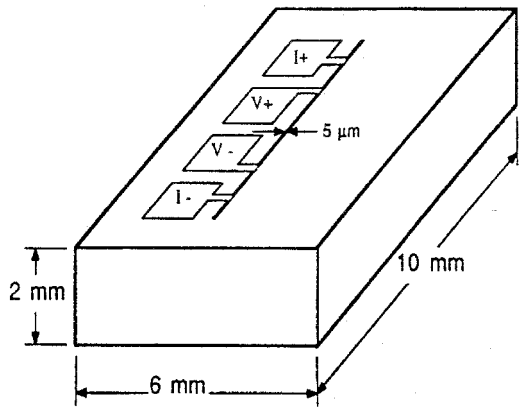

Fig. 2 Evaporated metal pattern produced on the face of a sample used for the 3v technique.[7]

Cahill et al.[7] reviewed the measuring techniques used for determining the thermophysical properties of thin films. The paper describes three methods, each being used for different film thicknesses. For film thicknesses of 10 μm and greater, Cahill and Pohl[8] developed an ac technique, designated as the 3ω technique, to measure the thermal conductivity and the specific heat. A thin, evaporated metal strip with four pads was used to measure the current and voltage, and was also used as a heater and thermometer because of the temperature-dependent electrical resistance of the metal strip. Figure 2 shows the evaporated metal pattern produced on the face of a sample used for the 3ω technique. The ac current with an angular frequency of ω causes a temperature wave of 2ω to diffuse into the substrate. The depth of penetration of this wave q^{-1} and the expression for thermal conductivity are given in Table 1.

The temperature amplitude ΔT of the heater was found to be inversely proportional to the thermal conductivity of the substrate and to the logarithm of the reciprocal angular frequency. By measuring ΔT as a function of ω, K can be directly determined. To measure the thermal conductivity of near-surface regions or films on substrates, the angular frequency ω is increased. If the heater–thermometer is evaporated onto a film of thickness d, on a substrate, the temperature wave will be confined to the film if $|q^{-1}| < d$. The measurement of thermal conductivity of thin films on substrates by this technique is highly dependent on the bonding between the film and the substrate.

A technique that enabled the measurement of thermal conductivity of films thinner than 100 Å, at the Laboratory of Atomic and Solid State Physics at Cornell University, was originally developed by Swartz and Pohl[9] to measure the thermal resistance at the interface of two solids. Figure 3 shows the experimental setup used in this technique. Two metal strips 2 μm apart are vapor-deposited onto a dielectric substrate. The electrical resistance of the metal strips is temperature-dependent, hence, the strips may be used as thermometers. The interface of interest is the one between the metal strip and the substrate. A large sensing current is induced in one of these metal strips and is used to measure its electrical resistance and hence its temperature. Further, the current causes the temperature of the metal strip to be higher than that of the substrate. The thermal resistance at the metal strip–substrate interface is given by the expression in Table 1.

The temperature of the dielectric substrate was determined by using the second metal strip as a thermometer and by inducing a smaller current. The difference in temperature between the second metal strip and the substrate underneath the first metal strip is calculated by integrating the Laplace equation for the geometry shown in Fig. 3. Knowing the thermal resistance at the interface, the thermal conductivity of the film may be determined. Cahill and Pohl[8] claim that this technique may be used to assess the quality of bonding between weakly adhering films to substrates.

Lee et al.[10] measured the thermal conductivity of a wide range of oxide thin films deposited by different sputtering techniques, using the 3ω technique. The thermal conductivity of SiO_2 films deposited by dc and rf magnetron sputtering on α–SiO_2 and SiO_2 substrates as a function of temperature is shown in the Results section. The experimental data obtained indicate a 20% reduction from bulk value and show little dependence on deposition technique or substrate used. For both Al_2O_3 and SiO_2, the thermal conductivity decreases with a decrease in temperature.

Lee et al.[10] also measured the thermal conductivity of titanium and magnesium oxides (TiO_2 and MgO). The thermal conductivity of these oxide films is shown as a function of temperature in the Results section. The paper concludes that the thermal conductivity of the amorphous oxide thin films Al_2O_3 and SiO_2 were comparable to bulk amorphous oxides, whereas microcrystalline thin films (TiO_2) may possess thermal conductivity values ranging from low values characteristic of

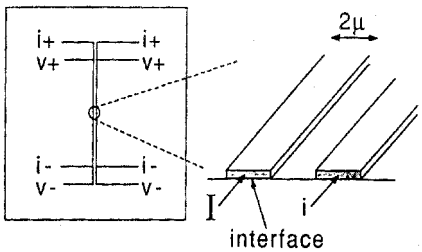

Fig. 3 Experimental geometry to determine the thermal resistance at solid interfaces.[8]

heavily disordered crystals to high thermal conductivities characteristic of bulk materials.

Cahill et al.[11] measured the thermal conductivity of sputtered α–Si:H thin films for a hydrogen content of 1–20% and film thickness of 0.2–1.5 μm over a temperature range of 80–400 K. A modification of the 3ω technique was used for this purpose. Five samples of α–Si:H of different hydrogen content were deposited on either a MgO or Si substrate. Although the results indicate that the lowest-hydrogen-content film does have the highest thermal conductivity, there does not appear to be a strong dependence on hydrogen content. The thermal conductivity as a function of temperature for the sample with a 1% hydrogen content is shown in the Results section. The paper also makes a comparison with theoretical results of Feldman et al.,[12] who invoked scattering of phonons by tunneling states to produce a finite mean free path for low-frequency phonons. Cahill et al.[11] modified this theory by including the contribution of thermal conductivity from vibrational modes of energies less than 10 meV. The results obtained indicate a favorable match between experimental and theoretical values.

Subsequently, Lee and Cahill[13] measured the thermal conductivity of 8 to 200-nm-thick films of SiO_2 and MgO over a temperature range of 78–400 K, using the 3ω technique. The apparent thermal conductivity of the thin films was extracted from the finite thermal conductance of the interfaces between the metal film heater and the dielectric layer, and between the dielectric layer and the silicon substrate.

The apparent thermal conductivity values obtained for both SiO_2 and MgO show a dependence upon temperature. For the plasma-enhanced, chemical-vapor-deposited (CVD) SiO_2, the apparent thermal conductivity slightly increases with an increase in temperature. A similar trend was observed for the MgO, with a maximum thermal conductivity value being obtained that is close to room temperature.

In both cases, the apparent thermal conductivity decreases with a decrease in film thickness. Thermal conductivity data for SiO_2 films thicker than 150 nm are only slightly lower than bulk values.

Zhang and Grigoropoulos[14] used a microbridge method to measure the thermal conductivity of a heavily doped, freestanding polycrystalline silicon film. The experimental setup is shown in Fig. 4. A steady-state heat flux is generated by passing a dc current in a heater placed at the center of the freestanding film. The temperature at the edge of the thin film has been assumed to be room temperature T_0. The sensor, which is a thin metal strip whose resistivity varies with temperature, is located at a distance X. The edge of the freestanding thin film is located at a distance L. The change in voltage across the sensor corresponds to the temperature change of the film at the sensor location. By measuring the heat flux q at the heater and ΔT at the sensor, the thermal conductivity of the thin film was determined. The expression obtained by Zhang and Grigoropoulos[14] relating the thermal conductivity is given in Table 1.

The thickness of the thin films was measured by three different techniques: 1) the phase shift method, 2) the amplitude method, and 3) the pulse method. The data obtained are shown as a function of temperature in the Results section. Between

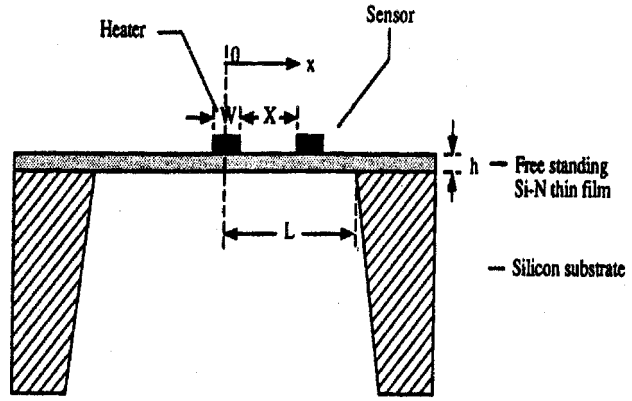

Fig. 4 Schematic of a freestanding Si–N thin film with a microheater and microsensor.[14]

300 and 400 K, the thermal conductivity remains constant, with the Si–N film 0.6 μm in thickness having a slightly higher thermal conductivity value.

The thermal comparator technique of measuring thermal conductivity was originally developed for bulk solids; Powell[15] published an extensive review on the subject. The procedure involves placing a hot thermocouple junction sensing tip into contact with a colder sample surface. A voltage, generated as a result of the temperature difference between the sensing tip and the reference junction, is recorded by a control module consisting of a personal computer. Several such voltages are recorded, averaged, and stored. Thermal conductivity calibration curves are generated for materials of known thermal conductivity, and by comparing materials of unknown thermal conductivity, the thermal conductivity may be determined. Figure 5 shows a schematic of the apparatus for this procedure.

The thermal comparator may also be used to measure the thermal conductivity of thin films applied on substrate materials. Lambropoulos et al.[16] presented an analytical model to determine thin-film thermal conductivity using this method, knowing the thermal conductivity of the substrate material. The model treats the film–interface–substrate as a semi-infinite body of apparent thermal conductivity K_{app}, where K_{app} is directly measured by the thermal comparator. The thin-film effective thermal conductivity K_{eff}, which includes interfacial effects between the film and the substrate and between the film and the probe tip, is determined using expressions presented in Table 1. The thin-film thermal conductivity is extracted as the slope of the straight line for the plot of t/K_{eff} as a function of film thickness t.

The methodology just discussed has the following limitations:

1) If K_{app} is close to the thermal conductivity of the substrate K_s, the resolution of the expression for K_{eff} becomes poor. For this reason, films that possess thermal conductivities close to that of the substrate may not be accurately tested.

2) The expression for K_{eff} is based on the fact that the substrate area is assumed to be a semi-infinite half space. This requires the films to be deposited on large substrates that may be considered as perfect heat sinks.

3) Application of load to ensure good contact between the probe and the film compresses the probe tip into the film–substrate sample and may cause localized thinning.

Völklein[17] determined the thermal conductivity of low-pressure, CVD, multilayer composite or sandwich SiO_2–Si_3N_4 films over a temperature range of 80–400 K. A steady-state technique utilizing a thin and very small stripe of an electrically conducting material deposited on the film is used for this purpose. The thin stripe, known as a bolometer, is heated by ac. The authors relate the rise in temperature of the bolometer to the thermal conductivity of the thin films. The measured value of thermal conductivity of the sandwich system at room

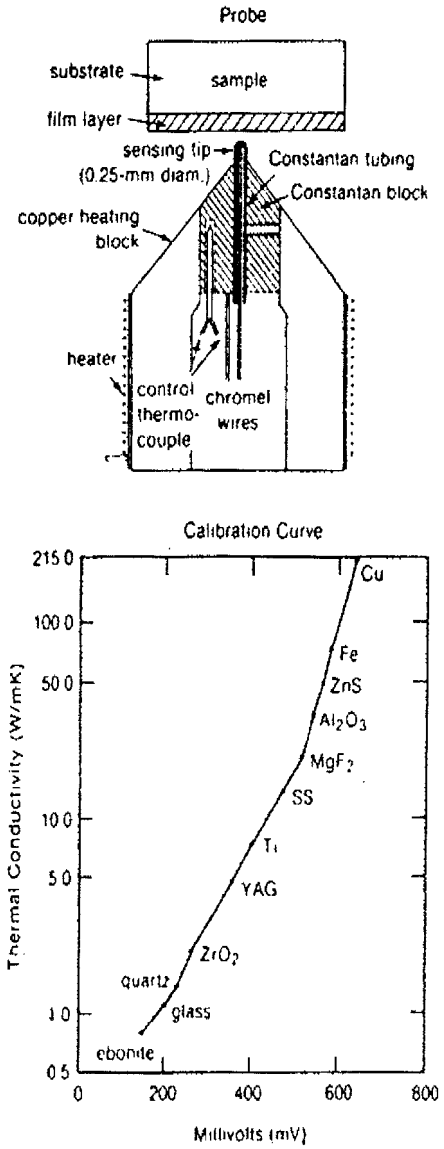

Fig. 5 Principle of operation of a thermal comparator.[16]

temperature was 2.4 W/mK. This differs significantly from bulk values of 12 and 17 W/mK for SiO_2 and Si_3N_4, respectively. This reiterates the discrepancies that exist between bulk and thin-film thermal conductivity values.

Völklein and Kessler[18] used the bolometer technique developed by Völklein[17] to measure the thermal conductivity of bismuth films ranging in thickness from 20–400 nm. As indicated in the Results section, the thermal conductivity of the bismuth films decreases with a decrease in thickness. This phenomenon is more pronounced at lower temperatures (100 K), where the differences are more significant. If we compare the bulk and thin-film thermal conductivity values for bismuth, the difference is significant at lower temperatures, but with an increase in temperature the values are closer because of the drastic drop in bulk thermal conductivity. The bulk and thin-film thermal conductivity values are approximately equal at 400 K (7 W/mK).

Stark et al.[19] also utilized the method developed by Völklein[17] to determine the thermal conductivity of aluminum oxide films deposited by anodic oxidation. The measurements were made at temperatures ranging from 90 to 350 K. The thermal conductivity ranged from 0.5 W/mK at 90 K to approximately 2.0 W/mK at 340 K.

Schafft et al.[20] also studied the thermal conductivity of thin SiO_2 films. The facilities used in determining the thermal conductivity were either a 400-μm-long straight-line metal structure or a cross-bridge structure. Both structures were equipped with four terminals to permit resistance measurements. The thermal conductivity of thin SiO_2 films were calculated from the measured joule heating and the temperature drop across the thin film.

The paper reports the thermal conductivity values for two thicknesses (1.74 and 3.04 μm) of phosphorus-doped silicon dioxide. A comparison with bulk thermal conductivity values indicates that the data obtained for the films are significantly lower. Further, the thermal conductivity decreases with increasing temperature. This trend is opposite to the temperature dependence reported by Lee et al.[10] The paper suggests that boundary scattering of phonons conducting the heat energy may be the reason for reduced thermal conductivity values and dependence on thickness of the film.

Brotzen et al.[21] determined the thermal conductivity of silicon dioxide films of four thicknesses deposited by plasma-enhanced chemical vapor deposition (PECVD) on monocrystalline silicon substrates. Figure 6 shows a sketch of the test specimen. A constant dc was passed through the aluminum stripe and the voltage drop was measured. For each current level, the temperature of the aluminum stripe and the silicon heat sink, the current, and the voltage were recorded. To eliminate directional thermocouple effects, the current direction was reversed after each measurement. By knowing the heat input and the temperature drop, the thermal conductivity of the thin film was determined.

The results obtained by Brotzen et al.[21] indicate that the thermal conductivity slightly decreases with increasing temperature. Further, the paper also indicates that different manufacturing–deposition methods create differences in thermal conductivity values. It is evident from the data obtained by Brotzen et al. that SiO_2 deposited by a two-pass intermediate air exposure PECVD operation possesses a lower thermal conductivity value compared with SiO_2 deposited by a continuous PECVD operation. The paper concludes that the thermal conductivity of SiO_2 films is sensitive to the technique employed in their deposition because the latter affects the physical and chemical nature of the film.

Goodson et al.[22,23] studied the annealing temperature dependence on thermal conductivity of low-pressure chemical-vapor-deposited (LPCVD) SiO_2 layers. The paper reports the effective thermal conductivity of undoped LPCVD, thermally grown (TG), and separation-by-implantation-with-oxygen (SI-

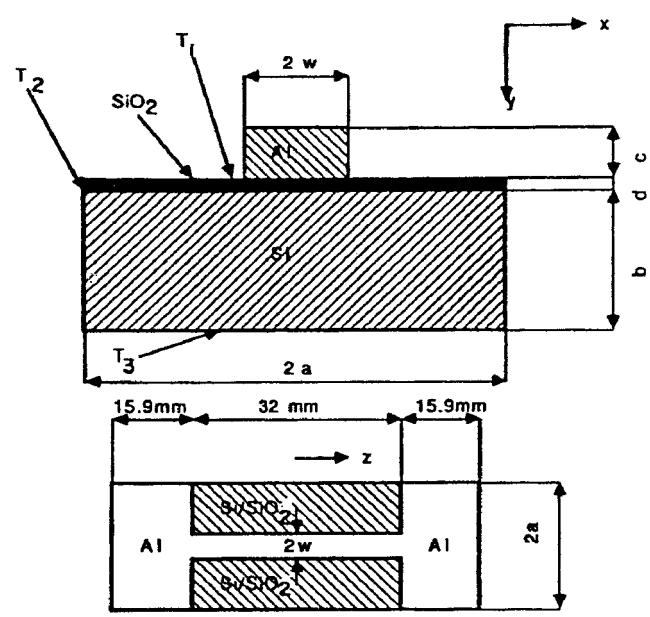

Fig. 6 Sketch of test specimen.[21]

MOX) SiO_2 layers on silicon substrates. The measurement technique utilized was the one developed by Goodson et al.,[22] based on the method of Swartz and Pohl.[9] The data obtained indicate that the effective thermal conductivity for LPCVD SiO_2 films increases with thermal processing temperature, at a given layer thickness.

Käding et al.[24] measured the thermal conductivity of TG and CVD silicon-dioxide layers 20–200 nm thick by using a noncontact, photothermal technique. Figure 7 shows the experimental geometry for the thermoreflectance measurements. The thermal resistance R_{th}, which is represented by an expression in Table 1, is assumed to consist of an internal volume resistance of the oxide layer d/k_{int}, and boundary resistances between the silicon dioxide and the silicon R_{B1} and between the silicon dioxide and the metal R_{B2}.

By measuring these thermal resistances, the internal thermal conductivity of the SiO_2 layers was calculated. The data presented in the Results section show a thickness independence and are lower than fused silica values. This may be attributed to the presence of impurities in the silicon-dioxide layers.

With the progressive increase in electronic packaging densities, synthetic diamond films are being used as heat spreaders. One of the attractive properties of bulk diamond is its very high thermal conductivity, which in single-crystal form can be as high as 2200 W/mK at room temperature. Further, at room temperature, diamond acts as an excellent thermal conductor and electrical insulator. Unfortunately, the thermal conductivity of diamond films may vary by factors of 3 to 5 (Ref. 25) for samples prepared by different techniques.

Graebner et al.[25] developed a technique to measure the thermal conductivity of CVD diamond films on silicon. The method involved the deposition of thin-film heaters and thermocouples on the surface of the diamond film by standard evaporation techniques using shadow masks. The silicon substrate was etched away completely in a small area, leaving a window of freestanding diamond. The dimensions of the window were critical to minimize radiative losses. The benefits of this technique are that it requires relatively small test specimens and small radiation losses, and it is not very complicated. The thermal conductivity of the diamond films as a function of film thickness is shown in the Results section. The data show a peak at a film thickness of 7.0 μm. The range of thermal conductivity values obtained was comparable to that of copper. Furthermore, compared to diamond in the single-crystal form, the thermal conductivity data show a decrease by approximately a factor of 6.

Graebner et al.,[26] in a subsequent publication, reported unusually high thermal conductivity values for diamond films of different thicknesses that were deposited on silicon under similar conditions. The thermal conductivity was measured by a technique described by Berman.[27] The local thermal conductivity values as a function of distance from the initial layer are shown in the Results section. Because the measured thermal conductivity value is an average over the entire thickness of the specimen, the data implies that the local thermal conductivity near the top surface of the 355-μm thick specimen is considerably higher than the measured average value. The paper also reports the variations of thermal conductivity as a function of grain size. The authors attribute the observed gradient in thermal conductivity to the phonon scattering by the roughly cone-shaped columnar microstructure.

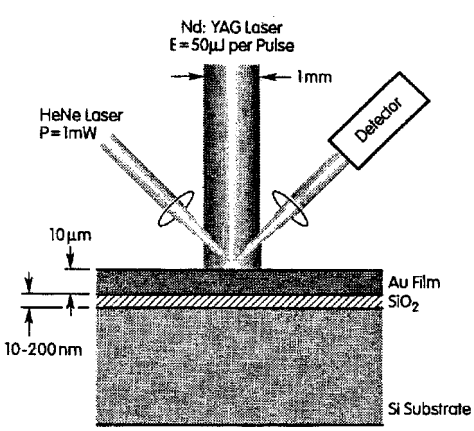

Fig. 7 Experimental geometry for thermoreflectance measurements.[24]

An important parameter that affects the thermal conductivity of polycrystalline diamond films is its microstructure. Graebner et al.[28] developed a laser technique[29] that enabled the thermal conductivity measurement of polycrystalline diamond films in a direction perpendicular to the plane of the diamond film. The diamond films were nucleated and grown on commercially available single-crystal silicon substrates by microwave-enhanced plasma CVD. The average thickness of these films was 28.4, 69.1, 185, and 408 μm. The measured and deduced local thermal conductivity data in a direction perpendicular to that of the film are presented in the Results section as well. The authors were able to extract the local thermal conductivity by comparing films of successive thickness. The maximum local thermal conductivity value of 2500 W/mK at 298 K is comparable to the value obtained for diamond in the single-crystal form. A comparison between the local thermal conductivity in directions parallel and perpendicular to the film shows that the rate at which they increase, with an increase in sample thickness, varies. This indicates anisotropy in the local thermal conductivity.

To understand these data, we recall that the phonons carrying heat energy are scattered by several mechanisms, including 1) impurities, 2) other high-energy phonons, 3) lattice defects, and 4) boundaries.[28,29] The first three mechanisms contribute approximately twice the amount of resistance attributable to boundary resistance, and the effect of all four mechanisms diminishes with an increase in film thickness. This partially explains the decrease in thermal conductivity gradient with an increase in temperature. The anisotropic behavior, on the other hand, is a little more difficult to explain. Transmission electron microscopy[30] studies show that lattice imperfections have a tendency to concentrate at grain boundaries, and would probably reflect incident phonons, instead of scattering them isotropically. This would result in a greater decrease of heat transport in the parallel direction compared with the perpendicular direction.

By assuming that defects are concentrated near grain boundaries, Goodson[31] related the internal phonon scattering to the local characteristic dimensions in diamond layers. It is evident from the results obtained that the conductivity of layers with larger grains increases far more rapidly with increasing layer thickness. Further, the data show that the thermal conductivity values predicted by Goodson[31] are significantly lower than that for high-quality, thick CVD diamond layers. This reduction is more prevalent at 77 K, because of the phonon mean free path being small from scattering at grain and layer boundaries, as well as the specific heat being lower compared with the value at room temperature. These phenomena cause the thermal conductivity of the diamond layers at 77 K to be less than half the value at room temperature.

Analytical Models

An empirical relationship for the thermal conductivity of dielectric materials was presented by Ziman.[32] The expression (Table 2) relates the thermal conductivity to the phonon specific heat per unit volume C, ν, and λ. At room temperature and above, λ varies inversely with temperature, but at low temperatures, λ varies exponentially with temperature. To deduce the thermal conductivity from the mean free path, the mean velocity ν is regarded as constant. At high temperatures, C is nearly constant, but as the temperature decreases, C also decreases and eventually varies as T^3, but the exponential

variation in ν is dominant, and K varies exponentially. When the mean free path of the phonons is constant, the thermal conductivity variation reflects the T^3 behavior of the specific heat.

Anderson[33] reported the electrical conductivity of rare-Earth transition metal (RETM) thin films deposited by vacuum sputtering. The electronic contribution to the thermal conductivity of RETM films was deduced by using the Wiedemann–Franz law, which is given in Table 2. The lattice contribution was estimated to be one-third the electronic contribution. The sum of these two components was considered to be the total thermal conductivity value.

Kittel[34] argues that the lattice contribution to thermal conductivity arises because of the heat conduction by quasiparticles, and may be expressed as given by Ziman.[32] Table 3 reports the electrical component, lattice contribution, and total thermal conductivity of four RETM thin films as determined by Anderson.[33] The paper concludes that the thermal conductivity values estimated by this method are one order of magnitude lower than bulk values.

Redondo and Beery[35] developed two models to explain the lower thermal conductivity of thin-film materials when compared with the bulk form of the same material. The first model developed by the authors, known as the microcrack model, postulates that the decrease in thermal conductivity is caused by the presence of microcracks. It is assumed that these microcracks possess a lower thermal conductivity than the coating. A schematic of the microcrack model is shown in Fig 8. The model predicts the ratio of the net thermal conductivity to the theoretical thermal conductivity of the film, as given by the expression in Table 2. Because the term in brackets is always equal to or greater than unity, we have $K_n \leq K$. Expressions represented in Table 2 may be used to predict the ratio of thermal conductivities for different values of α', β, and γ. It is evident that the net thermal conductivity decreases with a decrease in crack thermal conductivity.

Table 3 Thermal conductivity of RETM thin films[33]

Material	K_{el}, W/mK	K_{lat}, W/mK	K_{total}, W/mK
$Gd_{23}Co_{77}$ (planar magnetron)	2.8	0.8	3.6
$Tb_{24}Co_8Fe_{68}$ (ion beam)	3.8	1.1	4.9
$Tb_{21}Co_{10}Fe_{66}$ (triode magnetron)	4.9	1.4	6.4
$Gd_{15}Tb_{10}Co_9Fe_{66}$ (triode magnetron)	3.3	1.0	4.3

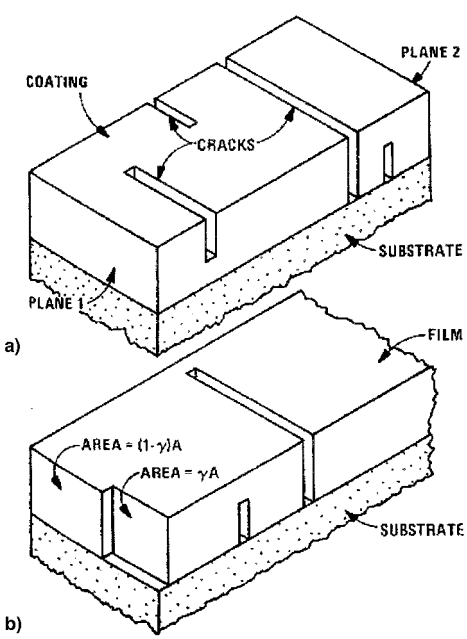

Fig. 8 Microcrack and Swiss cheese models.[35]

The second model developed by Redondo and Beery[35] accounts for the presence of randomly distributed voids throughout the film. This model was referred to as the Swiss cheese model, a schematic representation of which is also shown in Fig. 8. The ratio of the net thermal conductivity to the theoretical thermal conductivity as predicted by this model is given by the expression in Table 1. In this case as well, the ratio of the thermal conductivity is less than or equal to unity. A comparison of the two models indicates that microcracks can cause reductions of two or more orders of magnitude in the thermal conductivity of the film, whereas the presence of voids causes only a slight reduction in thermal conductivity.

Swimm[36] published a paper on the photoacoustic determination of thin-film thermal properties. This technique allows the individual determination of thermal conductivity and thermal diffusivity, from which the heat capacity per unit volume may be calculated. The thin-film measurement is conducted under conditions of substrate thickness >> substrate diffusion length, and thin-film thickness >> thin film optical depth. The author defines f_c, which is the chopping frequency above which the photoacoustic signal is independent of substrate effects, as given in Table 1.

The analysis proceeds by determining g and f_c from the experimental data, and then calculates the thin-film thermal conductivity and diffusivity in terms of g, f_c, thin-film thickness l_f, and the known substrate bulk thermal properties of k, ρ, and C_p. Here, g and f_c are calculated by measuring the phase differences using front-surface and rear-surface illumination.

Several researchers developed structure zone models by examining thin films using optical and electron microscopy techniques. These zone models categorize regimes of film growth by sorting the deposition conditions into regimes or zones where a relatively small number of physical processes dominate, and particular microstructures generally result.[37–39]

The original zone model for evaporated coatings was proposed by Movchan and Demchishin,[40] which was subsequently extended to magnetron sputtering. Three zones were categorized on the basis of the ratio of the substrate temperature T to the coating melting temperature T_m. They propose that zone 1, $T/T_m < 0.3$, results in a columnar structure consisting of tapered units defined by void boundaries; zone 2, $0.3 \leq T/T_m \leq 0.5$, results in a columnar structure with metallurgical boundaries; and zone 3, $T/T_m > 0.5$, results in grains of equal size.

Sanders[41] suggested a five-zone model, which, for below the melting point, includes essentially the three zones described by Movchan and Demchishin,[40] although the T/T_m ranges are different. Thornton[42,43] extended the zone model to magnetron-sputtered metal films by adding an axis to account for the

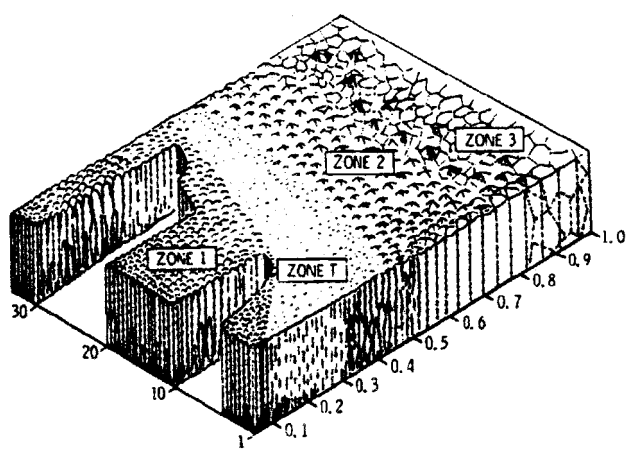

Fig. 9 Structure–zone diagram for metal films deposited by magnetron sputtering.[37]

effect of the argon working gas pressure (Fig. 9). A fourth zone consisting of fibrous grains was identified in the region between zones 1 and 2 and was termed zone *T*, as it was considered to be a transition zone.

Kim et al.[44] and Müller[45] performed computer simulations to predict the development of zones in film deposition techniques. Their results have provided a greater confidence level in the physical interpretations of the zone models.

Results

This section of the paper presents thin-film thermal conductivity data for the array of materials investigated. Figure 10 shows the data for the thermal conductivity of SiO_2, Si:H (1%), and the Si_3N_4 sandwich system. It is evident from Fig. 10 that SiO_2 deposited by rf and dc techniques[10] has a higher thermal conductivity than that of PECVD SiO_2.[13,21] Further, the thermal conductivity of phosphorus-based SiO_2 is comparable to data for PECVD SiO_2.[20] All these data are slightly lower than the bulk SiO_2 value. On the other hand, Si:H (1%) and the Si_3N_4 sandwich system possess a thermal conductivity higher than the bulk value.

Figure 11 shows the thermal conductivity of SiO_2 as a function of the thickness of the film. The data obtained by Okuba and Ohkubo[6] are comparable to those for bulk thermal conductivity values. Furthermore, it is evident that CVD SiO_2 appears to possess a slightly lower thermal conductivity value than the TG SiO_2 specimens.[24] Figure 11 also shows that the thermal conductivity data for thermal and SIMOX samples are extremely close to the bulk SiO_2 value.[22] This is contradictory to all the existing data for SiO_2 layers manufactured using other techniques. The difference in results reported by Goodson et al.[22] and Lambropoulos et al.[16] is possibly because of

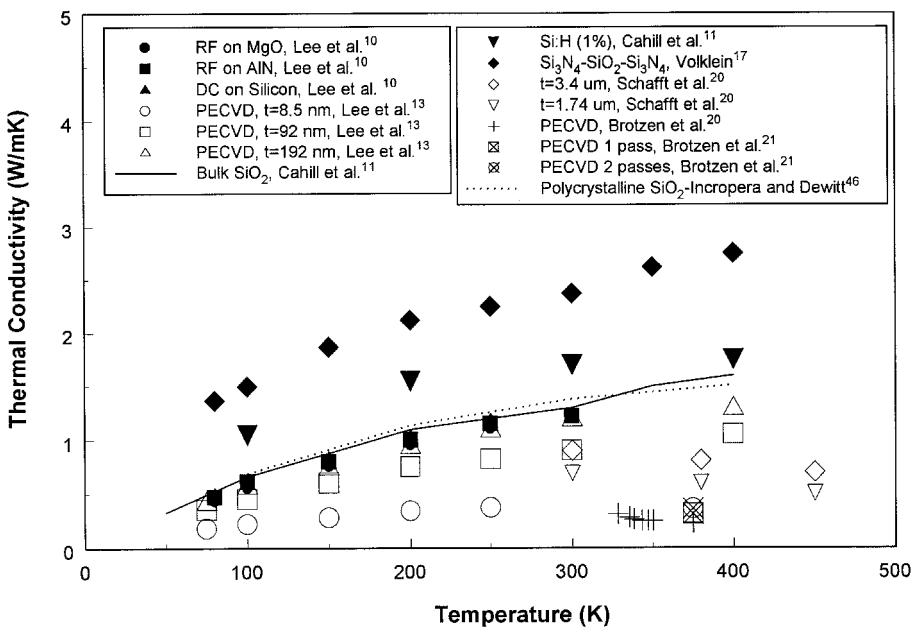

Fig. 10 Thermal conductivity of SiO_2, Si:H (1%), and the Si_3N_4 sandwich system as a function of temperature.

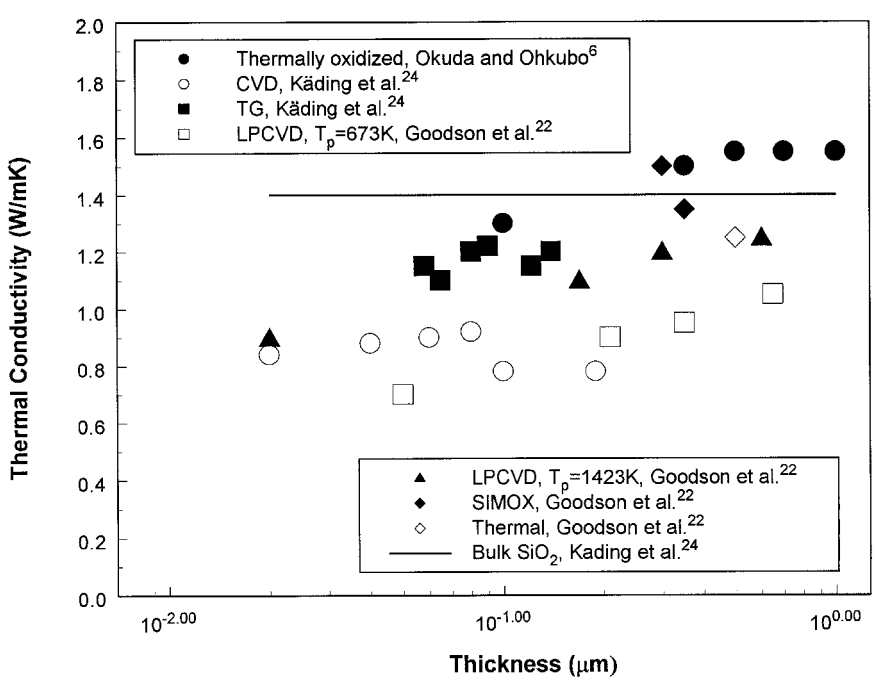

Fig. 11 Thermal conductivity of SiO_2 as a function of film thickness.

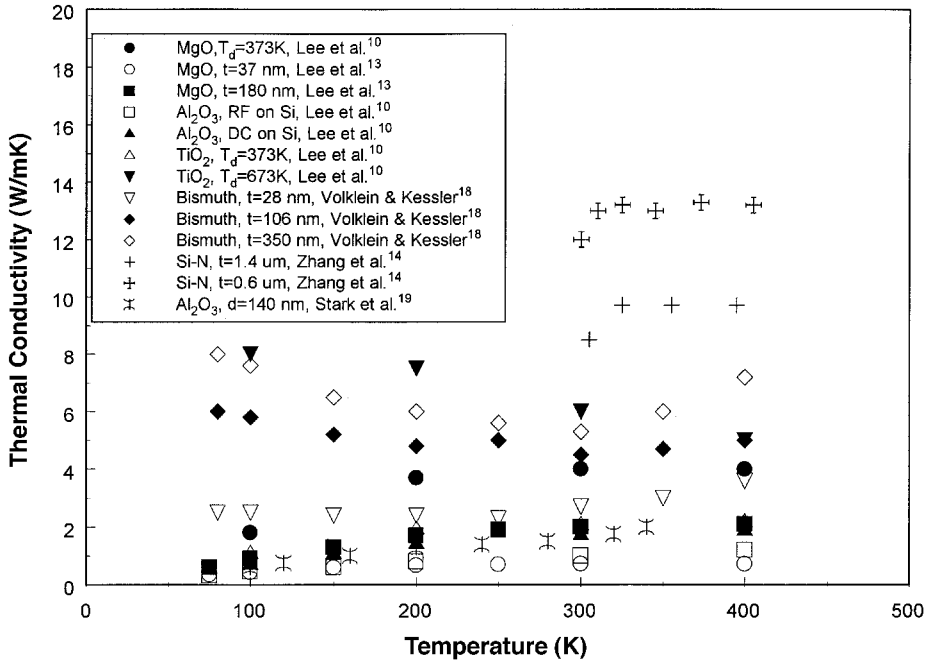

Fig. 12 Thermal conductivity of several different thin-film materials as a function of temperature.

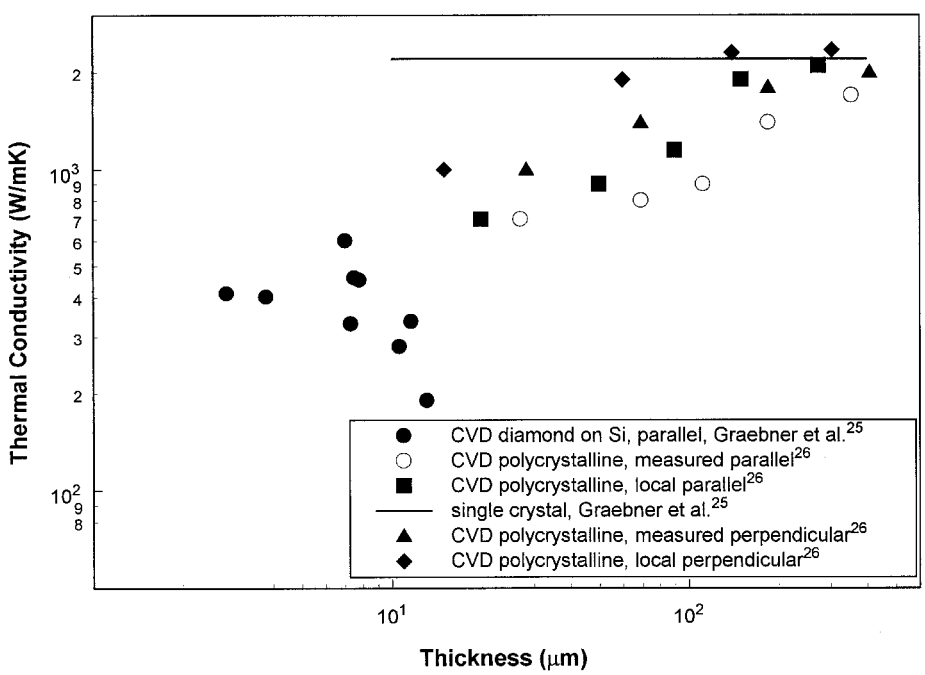

Fig. 13 Thermal conductivity of diamond films as a function of thickness.

the difference in deposition techniques (LPCVD vs ion and electron beam sputtering). A comparison of data obtained by Goodson et al.[22] and Brotzen et al.[21] (PECVD SiO_2) clearly indicates that the fabrication process strongly influences the thermal conductivity of SiO_2 thin films.

Figure 12 indicates the thermal conductivity data for several different thin-film materials. It is evident that the thermal conductivity of TiO_2 is extremely dependent upon the substrate temperature.[10] The thermal conductivity of MgO, on the other hand, is nearly independent of substrate temperature.[10] The thermal conductivity data for aluminum oxide show a significant difference between films deposited by dc and rf sputtering techniques.[10] Figure 12 also indicates that, with an increase in temperature, the thermal conductivity of the SiO_2–Si_3N_4 sandwich system increases, whereas the thermal conductivity of Si–N appears to be temperature independent.[14]

Figure 13 shows the thermal conductivity of bulk and diamond films as a function of thickness. The thermal conductivity of CVD diamond, in the parallel and perpendicular directions, increases with an increase in thickness and approaches single-crystal values. Figure 13 also indicates that the thermal conductivity of thin diamond films is lower than for thicker polycrystalline films.

Conclusions and Recommendations

Several different experimental and analytical techniques used to measure the thermal conductivity of thin films have been described. A comparison of the results obtained by these different techniques has also been made. This review also discusses several models that have been developed to predict and categorize the microstructure of films deposited on substrates. It is apparent that the thermal conductivity of thin-film mate-

rials is extremely dependent upon several parameters, which include film thickness, film and substrate temperature, and temperature and method of thin-film deposition. Therefore, it is critical that thermal conductivity measurements be made on samples that possess similar microstructures to those used in specific applications.

With the development of new experimental techniques and analytical models to measure and predict the thermophysical properties of thin films, the field of microscale heat transfer is growing rapidly. Over the last decade, the thermal properties of several different thin-film materials have been determined, including materials such as metallic oxides, RETM, and diamond. Although these materials have technological applications, there is a significant need to investigate the thermal properties of new materials that possess properties that meet the needs of advancing technology. Further, new methods of film deposition have been developed, such as pulse laser deposition and metal organic decomposition. It would be extremely beneficial to focus future research on the microstructural characterization of new materials deposited by new techniques on substrates by using diffraction and electron microscopy techniques. Although a majority of the thin-film materials have been deposited on silicon, it would prove interesting to study the effect of different substrates on the thermal properties of the film. Another important aspect that needs to be considered is the problem of radiation. Radiation effects may be significant depending upon the nature of the heat source, the area of exposed film surface, the type of film (coating or freestanding), and the temperature of the film. Future work in this field should emphasize a detailed radiation analysis of the results. Finally, greater emphasis needs to be attributed to the uncertainty involved in both the thickness and thermal conductivity results. The uncertainty analysis is critical, because the positioning and measurement of the distances between sensing devices far exceeds the thickness of the film. Further, the accurate measurement of the heat flux in the sample is extremely critical because of the nature of the thin film.

References

[1]Cahill, D. G., "Heat Transport in Dielectric Thin Films and at Solid-Solid Interfaces," *Microscale Thermophysical Engineering*, Vol. 1, No. 1, 1997, pp. 85–109.

[2]Goodson, K. E., and Flik, M. I., "Solid Layer Thermal Conductivity Measurement Techniques," *Applied Mechanics Reviews*, Vol. 47, No. 3, 1994, pp. 101–112.

[3]Graebner, J. E., "Thermal Conductivity of CVD Diamond: Techniques and Results," *Diamond Films and Technology*, Vol. 3, No. 2, 1993, pp. 77–130.

[4]Blanchard, D. G., Marotta, E. E., and Fletcher, L. S., "A Survey of the Thermal Conductivity of Synthetic and Natural Diamond Materials," AIAA Paper 92-0708, Jan. 1992.

[5]Chen, G., and Tien, C. L., "Thermal Conductivities of Quantum Well Structures," *Journal of Thermophysics and Heat Transfer*, Vol. 7, No. 2, 1993, pp. 311–318.

[6]Okuda, M., and Ohkubo, S., "A Novel Method for Measuring the Thermal Conductivity of Submicrometre Thick Dielectric Films," *Thin Solid Films*, Vol. 213, May 1992, pp. 176–181.

[7]Cahill, D. G., Fischer, H. E., Klitsner, T., Swartz, E. T., and Pohl, R. O., "Thermal Conductivity of Thin Films: Measurements and Understanding," *Journal of Vacuum Science and Technology*, Vol. A7, No. 3, 1989, pp. 1259–1266.

[8]Cahill, D. G., and Pohl, R. O., "Thermal Conductivity of Amorphous Solids Above the Plateau," *Physical Review B: Solid State*, Vol. 35, No. 8, 1987, pp. 4067–4073.

[9]Swartz, E. T., and Pohl, R. O., "Thermal Resistance at Interfaces," *Applied Physics Letters*, Vol. 51, No. 26, 1987, pp. 2200–2202.

[10]Lee, S. M., Cahill, D. G., and Allen, T. H., "Thermal Conductivity of Sputtered Oxide Films," *Physical Review B: Solid State*, Vol. 52, No. 1, 1995, pp. 253–257.

[11]Cahill, D. G., Katiyar, M., and Abelson, J. R., "Thermal Conductivity of ∝-Si:H Thin Films," *Physical Review B: Solid State*, Vol. 50, No. 9, 1994, pp. 6077–6081.

[12]Feldman, J. L., Kuge, M. D., Allen, P. B., and Wooten, F., "Thermal Conductivity and Localization in Glasses: Numerical Study of a Model of Amorphous Silicon," *Physical Review B: Solid State*, Vol. 48, No. 17, 1993, pp. 12,589–12,595.

[13]Lee, S. M., and Cahill, D. G., "Influence of Interface Thermal Conductance on the Apparent Thermal Conductivity of Thin Films," 2nd U.S./Japan Molecular and Microscale Phenomena Conf., Univ. of California, Santa Barbara, CA, Aug. 1996.

[14]Zhang, X., and Grigoropoulos, P., "Thermal Conductivity and Diffusivity of Free Standing Silicon Nitride Thin Films," *Review of Scientific Instruments*, Vol. 66, No. 2, 1995, pp. 1115–1120.

[15]Powell, R. W., "Experiments Using a Simple Thermal Comparator for Measurement of Thermal Conductivity, Surface Roughness, and Thickness of Foils or of Surface Deposits," *Journal of Scientific Instruments*, Vol. 34, Dec. 1957, pp. 485–492.

[16]Lambropoulos, J. C., Jacobs, S. D., Burns, S. J., Shaw-Klein, L., and Hwang, S. S., "Thermal Conductivity of Thin Films: Measurements and Microstructural Effects," *Thin Film Heat Transfer: Properties and Processing*, Vol. 184, American Society of Mechanical Engineers, HTD, New York, 1991, pp. 21–32.

[17]Völklein, F., "Thermal Conductivity and Diffusivity of a Thin Film SiO_2-Si_3N_4 Sandwich System," *Thin Solid Films*, Vol. 188, July 1990, pp. 27–33.

[18]Völklein F., and Kessler E., "Methods for the Measurement of Thermal Conductivity and Thermal Diffusivity of Very Thin Films and Foils," *Measurement*, Vol. 5, No. 1, 1987, pp. 38–45.

[19]Stark, I., Stordeur, M., and Syrowatka, F., "Thermal Conductivity of Thin Amorphous Alumina Films," *Thin Solid Films*, Vol. 226, April 1993, pp. 185–190.

[20]Schafft, H. A., Suehle, J. S., and Mirel, P. G. A., "Thermal Conductivity Measurements of Thin Film-Silicon Dioxide," *Proceedings of the IEEE 1989 International Conference on Microelectronic Test Structures*, Vol. 2, No. 1, Inst. of Electrical and Electronics Engineers, New York, 1989, pp. 121–125.

[21]Brotzen, F. R., Loos, P. J., and Brady, D. P., "Thermal Conductivity of Thin SiO_2 Films," *Thin Solid Films*, Vol. 207, Jan. 1992, pp. 197–201.

[22]Goodson, K. E., Flik, M. I., Su, L. T., and Antoniadis, D. A., "Annealing Temperature Dependence of the Thermal Conductivity of LPCVD Silicon-Dioxide Layers," *IEEE Electron Device Letters*, Vol. 14, No. 10, 1993, pp. 490–492.

[23]Goodson, K. E., Flik, M. I., Su, L. T., and Antoniadis, D. A., "Prediction and Measurement of Thermal Conductivity of Amorphous Dielectric Layer," *Journal of Heat Transfer*, Vol. 116, May 1994, pp. 317–324.

[24]Käding, O. W., Skurk, H., and Goodson, K. E., "Thermal Conduction Normal to Metallized Silicon-Dioxide Layers on Silicon," *Applied Physics Letters*, Vol. 65, No. 13, 1994, pp. 1629–1631.

[25]Graebner, J. E., Mucha, J. A., Seibles, L., and Kammlott, G. W., "The Thermal Conductivity of Chemical Vapor Deposited Diamond Films on Silicon," *Journal of Applied Physics*, Vol. 71, No. 7, 1992, pp. 3143–3146.

[26]Graebner, J. E., Jin, S., Kammlott, G. W., Herb, J. A., and Gardinier, C. F., "Unusually High Thermal Conductivity in Diamond Films," *Applied Physics Letters*, Vol. 60, No. 60, 1992, pp. 1576–1578.

[27]Berman, R., *Thermal Conduction in Solids*, Oxford Univ. Press, Oxford, England, UK, 1976.

[28]Graebner, J. E., Jin, S., Kammlott, G. W., Herb, J. A., and Gardinier, C. F., "Large Inisotropic Thermal Conductivity in Synthetic Diamond Films," *Nature*, Vol. 359, Oct. 1992, pp. 401–403.

[29]Graebner, J. E., Jin, S., Kammlott, G. W., Bacon, B., Seibles, L., and Banholzer, W., "Anisotropic Thermal Conductivity in Chemical Vapor Deposited Diamond," *Journal of Applied Physics*, Vol. 71, June 1992, pp. 5353–5356.

[30]Hetherington, A. V., Wort, C. J. H., and Southwort, P. J., "Crystalline Perfection of Chemical Vapor Deposited Diamond Films," *Journal of Materials Research*, Vol. 5, Aug. 1990, pp. 1591–1594.

[31]Goodson, K. E., "Thermal Conduction in Non-Homogeneous CVD Diamond Layers in Electronic Microstructures," *Journal of Heat Transfer*, Vol. 118, May 1996, pp. 279–286.

[32]Ziman, J. M., *Electrons and Phonons; the Theory of Transport Phenomena in Solids*, Oxford Univ. Press, Oxford, England, UK 1960.

[33]Anderson, R. J., "The Thermal Conductivity of Rare-Earth-Transition-Metal Films as Determined by the Wiedemann-Franz Law," *Journal of Applied Physics*, Vol. 67, No. 11, 1990, pp. 6914–6916.

[34]Kittel, C., *Introduction to Solid State Physics*, Wiley, New York, 1996.

[35]Redondo, A., and Beery, J. G., "Thermal Conductivity of Optical Coatings," *Journal of Applied Physics*, Vol. 60, No. 11, 1996, pp. 3882–3885.

[36]Swimm, R. T., " Photoacoustic Determination of Thin-Film Properties," *Applied Physics Letters*, Vol. 42, No. 11, 1983, pp. 955–957.

[37]Thornton, J. A., "Structure-Zone Models of Thin Films," *Proceedings of the Society of Photo-Optical Instrumentation Engineers*, Vol. 821, SPIE, Bellingham, WA, 1987, pp. 95–103.

[38]Thornton, J. A., "High Rate Thick Film Growth," *Annual Review of Materials Science*, Vol. 7, 1977, pp. 239–260.

[39]Thornton, J. A., "The Microstructure of Sputter-Deposited Coatings," *Journal of Vacuum Science and Technology*, Vol. A4, No. 6, 1986, pp. 3059–3065.

[40]Movchan, B. A., and Demchishin, A. V., "Study of the Structure and Properties of Thick Vacuum Condensates of Nickel, Tungsten, Aluminum Oxide, and Zirconium Oxide," *Journal of Physics of Metals and Metallography*, Vol. 28, No. 4, 1969, pp. 83–90.

[41]Sanders, J. V., "Structure of Evaporated Metal Films," *Chemisorption and Reactions on Metal Films*," edited by J. R. Anderson, Academic, New York, 1971, pp. 1–38.

[42]Thornton, J. A., "Influence of Apparatus Geometry and Deposition Conditions on the Structure and Topography of Thick Sputtered Coatings," *Journal of Vacuum Science and Technology*, Vol. 11, No. 4, 1974, pp. 666–676.

[43]Thornton, J. A., "Microstructure Considerations in Hydrogenated Amorphous Silicon Thin Films," *Amorphous Metals and Semiconductors*, edited by P. Hassen and R. I. Jaffee, Pergamon, New York, 1986, pp. 299–314.

[44]Kim, S., Henderson, D. J., and Chaudhari, P., "Computer Simulation of Amorphous Thin Films of Hard Spheres," *Thin Solid Films*, Vol. 47, Nov. 1977, pp. 155–158.

[45]Müller, K. H., "Dependence of Thin Film Microstructure on Deposition Rate by Means of a Computer Simulation," *Journal of Applied Physics,* Vol. 58, No. 7, 1985, pp. 2573–2581.

[46]Incropera, F. P., and Dewitt, P. D., *Fundamentals of Heat and Mass Transfer*, 3rd ed., Wiley, New York, 1990.